Molecular Crystals and Liquid Crystals
Publication details, including instructions for authors and subscription information:
http://www.tandfonline.com/loi/gmcl16

Measurements of Soliton Trapping and Motion in Trans-Polyacetylene Using Dynamic Nuclear Polarization

W. G. Clark [a], K. Glover [a], G. Mozurkewich [a d], S. Etemad [b] & M. Maxfield [c]

[a] Physics Department, University of California at Los Angeles, Los Angeles, CA, 90024, USA

[b] AT & T Bell Laboratories, Whippany, NJ, 07981, USA

[c] Allied Chemical Corporation, Morristown, NJ, 07960, USA

[d] Physics Dept., Univ. of Illinois at Urbana-Champaign, Urbana, IL, 61801

Version of record first published: 17 Oct 2011.

To cite this article: W. G. Clark , K. Glover , G. Mozurkewich , S. Etemad & M. Maxfield (1985): Measurements of Soliton Trapping and Motion in Trans-Polyacetylene Using Dynamic Nuclear Polarization, Molecular Crystals and Liquid Crystals, 117:1, 447-454

To link to this article: http://dx.doi.org/10.1080/00268948508074663

Mol. Cryst. Liq. Cryst. 1985, Vol. 117, pp. 447-454
0026-8941/85/1174-0447/$15.00/0

Printed in the United States of America

MEASUREMENTS OF SOLITON TRAPPING AND MOTION IN TRANS-POLYACETYLENE USING DYNAMIC NUCLEAR POLARIZATION

W.G. CLARK, K. GLOVER, G. MOZURKEWICH*
Physics Department, University of California at Los Angeles, Los Angeles, CA 90024, USA

S. ETEMAD
AT&T Bell Laboratories, Whippany, NJ 07981, USA

M. MAXFIELD
Allied Chemical Corporation, Morristown, NJ 07960 USA

Abstract The motion of solitons in undoped trans-$(CH)_x$ is studied over the temperature range 1.5-300 K using dynamic nuclear polarization. The results of a theoretical model for the combined solid state and Overhauser effects in terms of the time dependence of the electron nuclear interaction due to motion of electrons is presented. Its application to the experiment shows that most of the solitons are trapped below 30 K and that the mobile solitons above 30 K have a diffusion coefficient that is approximately proportional to the square root of the temperature. At 300 K the time for a soliton to diffuse its length is greater than or equal to 1.7×10^{-11} seconds.

INTRODUCTION

The properties of solitons in trans-$(CH)_x$ have been a subject of intense study in recent years. According to the model[1] of a soliton in trans-$(CH)_x$, the neutral soliton has an unpaired spin, and can therefore be investigated through its magnetic properties. These include its susceptibility, spatial extent, motion, etc.

In this paper we report experimental and theoretical results aimed at studying trapping and motion of the unpaired electron spins in pristine trans-$(CH)_x$. (Because many of the properties of these spins are consistent with what is expected of solitons, we shall henceforth refer to them as such.)

The property we consider is the dynamic nuclear polarization (DNP) that occurs for the protons when the electron spin state populations are driven out of thermal equilibrium by a strong

microwave magnetic field. It is well known that this DNP, which reflects the interaction between the electron and nuclear spins, can be used as a microscopic probe of the soliton motion relative to the fixed protons in trans-$(CH)_x$. Prior work on this subject[2,3] has applied the idea that if the solitons are fixed (trapped) or moving very slowly, the DNP occurs via the solid state effect (SSE), whereas if it is rapid, the DNP is through the Overhauser effect (OE). Our theoretical results go beyond this earlier work in that they allow a detailed, quantitative, connection between a correlation function for the soliton motion and the DNP. It is discussed in the next section. The subsequent section then applies these results to measurements of the proton DNP over the temperature range 1.5-300 K.

The main conclusions of our work are that the solitons become trapped or bound over the temperature range 10 K $\lesssim T \lesssim$ 100 K, and that that they become progressively more mobile as the temperature is increased. From these experiments, it is also estimated that the diffusion constant for the rapidly moving solitons varies as $T^{1/2}$, and that a lower limit on the time for a soliton to diffuse its length at 300 K is 1.7×10^{-11} seconds.

THEORETICAL MODEL

In this section we present the results of calculations of the dynamic nuclear polarization (DNP) caused by unpaired electron spin motion in trans-$(CH)_x$. The standard four-level model of one electron with spin S=1/2 and one proton with I=1/2 is used.[4] Because of the low soliton concentration (N) in our sample ($N\approx3\times10^{-4}$ per formula unit), we assume that interelectron spin interactions play a negligible role in the DNP. This means that the model of our electron and one spin should be valid. The weak many-body aspects of the problem are folded phenomenologically into the ESR linewidth, and it is not necessary to invoke the more complex treatment that is appropriate when the interactions among the electron spins are stronger.[5] The main point of the calculation is to establish the basis for analyzing experiments quantitatively when both the OE and the SSE are present because of translational motion of the electron spin. Details of the calculation will be published elsewhere.

The formulae for analyzing our experiments are obtained with the following considerations. The model Hamiltonian used is

$$H = H_z + H_{e-n} + H_{rf} \tag{1}$$

where H_z is the Zeeman term for the electron and the nucleus, H_{e-n} is the electron-nuclear interaction, and H_{rf} is the interaction of the electron spin with the magnetic field of amplitude H_1 and frequency ω used to partially saturate the allowed and forbidden ESR transitions. When the electron spin moves, H_{e-n} becomes a

random function of time, with a correlation function G(t) that reflects the details of the electron motion. In particular, it is sensitive to such factors as the dimensionality of the motion, the time scale of the motion, and whether there is trapping of the electrons. Because of the short range nature of H_{e-n}, G(t) is simply the probability that if the electron is located at the nucleus at time t=0, it is there at a later time t. The effect of G(t) is to induce transitions between the energy levels of the system through its Fourier transform, the power spectrum $J(\omega_i)$, where ω_i is the frequency of the corresponding transition.

The DNP of the protons is obtained by solving the rate equations for the four level system. They include all relaxation transitions caused by motion of the electron relative to the nucleus, relaxation transitions of the electron via interaction with other reservoirs, and all rf-magnetic field-induced transitions that include one spin flip of the electron. The latter transitions are the allowed transition associated with the usual ESR signal, which is responsible for the OE, and the forbidden transition involving both an electron and a nuclear spin flip, which is responsible for the SSE. An important part of the calculation is to express this forbidden rate in terms of $J(\omega_i)$, as it contains much of the information needed to obtain conclusions about the microscopic details of the soliton motion.

The full solutions for the DNP are rather complicated. They can however, be simplified on the basis of reasonable assumptions, such as the electron magnetic moment being large compared to that of the nucleus. For the case of a single G(t) for all of the electrons, i.e., not two populations one trapped and one mobile, the following expressions are obtained for ε_s and ε_o, the SSE and OE enhancements factors, respectively.

$$\varepsilon_s = \left(\frac{\gamma_e}{\gamma_n}\right)\left(\frac{N}{n}\right)\frac{T_{1n}}{T_{1e}}\left(\frac{sF(\omega)}{1+sg(\omega)}\right) \tag{2}$$

$$\varepsilon_o = \left(\frac{\gamma_e}{\gamma_n}\right)\left(\frac{N}{n}\right)T_{1n}\left(\frac{sg(\omega)}{1+sg(\omega)}\right)AJ(\omega_e) \tag{3}$$

In Eqs. 2-3, γ_e and γ_n are the electron and nuclear gyromagnetic ratios, ω_e is the ESR frequency, T_{1n} and T_{1e} are the nuclear and electron spin-lattice relaxation times, $(\gamma_e T_{2e})^{-1}$ is the ESR linewidth (Δ), n is the concentration of nuclei, s is the ESR saturation factor $(\gamma_e^2 H_1^2 T_{1e} T_{2e})$, $g(\omega)$ is the ESR absorbtion lineshape, A is a combination of matrix elements of H_{e-n}, and the factor F is

$$F(\omega) = 2\pi\left(\frac{\gamma_e H_1}{\omega_n}\right)^2 \int_{-\infty}^{+\infty} d\Omega J(\Omega)\left(g(\omega-\omega_e+\omega_n-\Omega)-g(\omega-\omega_e+\omega_n-\Omega)\right) , \tag{4}$$

where ω_n is the NMR frequency and Ω is the variable of integration. There are several points to be made about the above results [we assume a symmetric $g(\omega)$]:

(a) The factor F, which controls the shape of the SSE, is a

convolution of $J(\omega_1)$ and the difference of the ESR absorption line shape $g(\omega)$ shifted to $\pm\omega_n$ about $\omega=0$.

(b) ε_s has odd symmetry about its center, which can be used to identify it.

(c) In order to obtain a quantitative comparison with experiments, other quantities, such as T_{1e}, T_{1n}, N, n, $g(\omega)$, and s must be known from other experiments or from calculations.

(d) For small $sg(\omega)$, ε_o has the shape of the ESR line itself. Even for larger $sg(\omega)$, it is easily distinguished from ε_s because it has even symmetry about the center of $g(\omega)$.

(e) In the above equations, we have assumed that dipolar coupling among the nuclear spins is strong enough to maintain them all at the same spin temperatures.

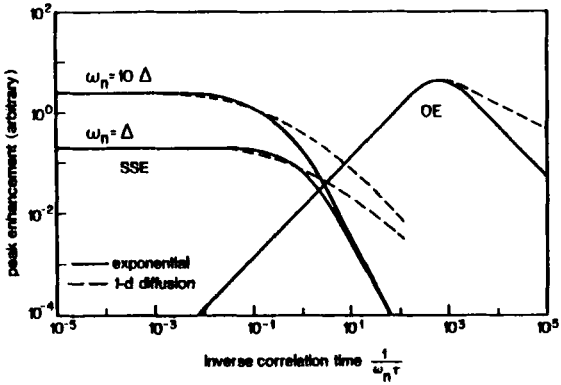

FIGURE 1 Theoretical values of the peak solid and Overhauser effects for different values of the ESR linewidth versus the inverse correlation time.

Figure 1 shows a plot of the peak value of ε (on an arbitrary scale) as a function of the jump rate τ^{-1} for two modes of the decay of G(t). One corresponds to an exponential decay, $G=e^{-t/\tau}$ (solid lines), and the other (dashed lines) is diffusion of a localized electron spin on a 1-d chain of finite length (ℓ). The jump rate is normalized to ω_n, a Lorentzian ESR lineshape of width Δ is assumed, and the nuclei are taken to be protons. Such graphs are useful, as they demonstrate the evolution of ε_s and ε_o as the electron goes continuously from no motion at all to progressively more rapid diffusion.

From Fig. 1, the following features can be seen:

(a) Substantial attenuation of the SSE occurs when $\Delta\tau \simeq 1$, and then continues rapidly as τ^{-1} increases further. This shows quantitatively the disappearance of the SSE as the electron motion becomes more rapid. The detailed nature of the disappearance reflects the model used for G(t), and is therefore sensitive to the dimensionality of the motion.

(b) The OE increases to a peak as τ^{-1} increases to ω_e, and then decreases as τ^{-1} becomes larger still. In the region $\omega_e\tau < 1$, $\varepsilon_o \propto \tau^{-1}$; i.e., it is insensitive to the dimensionality of the motion, as it is dominated by times less than the elementary hop time. The diffusion regime does not develop until $\omega_e\tau > 1$.

(c) Because of the large difference between ω_n and ω_e, the SSE disappears before the OE emerges, leaving a dip in the total enhancement.

In anticipation of our experimental results, we also consider the case in which there are two populations of solitons,[6] one that moves rapidly (concentration N_f) and one that is trapped, or moves very slowly (concentration N_s). Under these circumstances, the enhancement is written as the sum of the SSE and OE, but weighted by the concentrations of the two population:

$$\varepsilon = \frac{N_s\varepsilon_s+N_f\varepsilon_o}{N_s+N_f} \; ; \; N = N_s + N_f \; . \tag{5}$$

Various models can then be used for the dependence of N_s and N_f upon T.

EXPERIMENTAL METHODS AND RESULTS

The sample used in this work is the same as the sealed one described earlier.[3] Both the ESR signal at a fixed frequency of 9.3 GHz and the proton NMR signal amplitude were recorded simultaneously as the field was swept through the ESR line. The NMR oscillator frequency was synchronized with the field sweep so that the proton resonance condition was always satisfied. This was done first so that thermal equilibrium values were obtained. Then the measurement was repeated at a high microwave power level to generate the DNP signal. From the high-power ESR signal the value of s was obtained. The value of s was obtained from the increase in the ESR linewidth under high power excitation.

The DNP signal was often an asymmetric mixture of the SSE (odd about the center) and the OE (even about the center). These symmetry properties were used to decompose the total DNP signal into an SSE part and an OE part at each T. The results are shown in Figs. 2 and 3, where the peak normalized ε_s and ε_o (ε_{smax} and ε_{omax}) are plotted as a function of T. In calculating the normalization, published values were used for T_{1e}[7] and T_{1n}[3]. Both s and $g(\omega)$ were obtained in the present experiments. Representative errors in the reduced data are indicated by the scatter in the points.

The overall picture given by Figs. 2-3 is that there is a complete SSE at low T, a complete OE at high T, and a smooth crossover between the two centered near 30 K. This is in rough agreement with earlier work,[2,3] and confirms the idea that the solitons are fixed at low T, but become progressively more mobile at high T. The data of Figs. 2-3 can be compared with the models

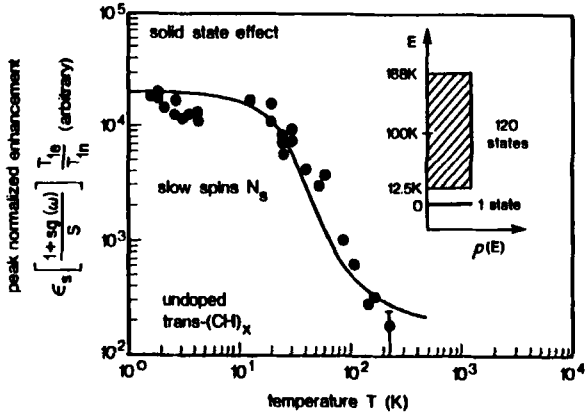

FIGURE 2 Experimental values of the normalized solid effect as a function of T compared to the theoretical number of bound electrons for a distribution of binding energies in a two population model.

shown in Fig. 1 through the assumption that τ is a function of T and that it becomes shorter as T increases. If the results of Figs. 2-3 are compared in this way with Fig. 1, it is seen that the dip in the peak enhancement between the disappearance of the SSE and the emergence of the OE does not occur in our experiments. This indicates that a G(t) with a single τ for all of the electrons does not apply. For this reason, we have turned to the two population model (trapped and mobile solitons) described at the end of the previous section.

There is an additional point to indicate that a two population model is appropriate. If the high T loss of the SSE were due to a smooth decrease in τ, Eq. 4 predicts that the field separation between the peaks of the SSE should increase substantially as ϵ_s decreases through the values shown in Fig. 2. We have carefully examined our SSE curves and find that no significant increase in this separation occurs. This means that all of the solitons giving rise to the SSE are immobile for a time $t > \omega_n^{-1} \cong 1.1 \times 10^{-8}$s, i.e., the solitons responsible for the SSE are trapped.

We have applied the model density of states ρ as a function of energy E shown in the upper right of Fig. 2 to simulate the observed SSE. It has one trapped state (N_s) at E=0 and 120 mobile states (N_f) distributed evenly over 12.5 K $\leq$ E $\leq$ 188 K. With these parameters, the solid curve in Fig. 2 is generated. Although this curve has several parameters, each of them affects the fit at a different temperature range. For this reason, we believe it represents the main features of soliton trapping.

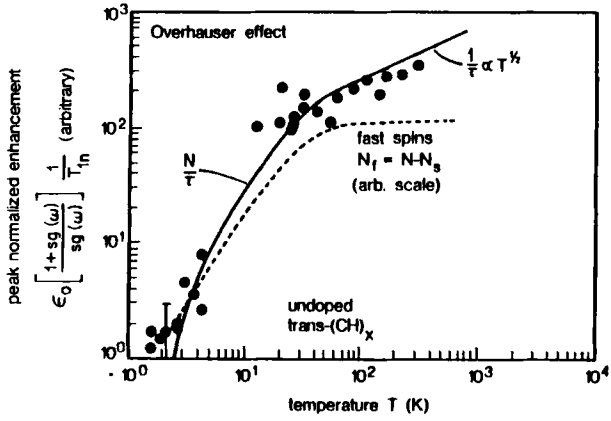

FIGURE 3 Experimental values of the normalized OE versus T compared to the theoretical curves of the number of fast solitons and the number of fast solitons divided by the correlation time, for a two population model with a distribution of binding energies.

Now we discuss the conclusions to be drawn from the OE (Fig. 3). We assume a fixed number of spins, as implied by the Curie-law susceptibility.[8] Then, the absence of a peak in the normalized enhancement means that (see Fig. 1) $\omega_e\tau > 1$. Analysis of the models for ϵ_o show that under these conditions, $\epsilon_{omax} \propto N_f\tau^{-1}$ over the entire temperature range studied. The temperature dependence of N_f alone is obtained from Eq. 5 and Fig. 2 and is shown by the dashed line in Fig. 3. The difference between it and the data reflect the temperature dependence of τ^{-1}. A reasonable fit to these data has been obtained by assigning $\tau^{-1} \propto T^{1/2}$, which is shown by the solid line. The quality of this fit over a wide range of T and ϵ_{omax} indicates that this power law behavior for τ^{-1} is a reasonably good description. The condition $\omega_e\tau \gtrsim 1$ implies that $\tau \gtrsim 1.7\times10^{-11}$ over the entire range of T including its shortest value at 300 K. Since it is the characteristic time for H_{e-n} to decay, it represents the time for a soliton to diffuse a distance the order of its length. If we take the length $\cong$ 15 lattice constants along the polymer chain[1] and assume the motion to be random jumps by one lattice constant, our results set an upper limit of $1.3\times10^{13}s^{-1}$ on the elementary jump rate. It is close to but somewhat less than the value reported from the electron[9] and nuclear[10] spin-lattice relaxation measurements. The reason for this difference is not yet clear.

CONCLUSION

In this paper we have reported the results of a model for dynamic nuclear polarization that permits a direct comparison with experiments in terms of the motion of electrons relative to the nuclei. Experimental results of the dynamic nuclear polarization in undoped trans-$(CH)_x$ are presented for the temperature range 1.5-300 K and analyzed using this theoretical model. This analysis shows that the solitons are trapped at low T, very mobile at high T, and that there is a gradual conversion from trapped to mobile populations over the range 10 K < T < 100 K. The mobile solitons have a diffusion constant whose temperature variation is given approximately by $T^{1/2}$. At all temperatures studied, the time for a soliton to diffuse its length exceeds 1.7×10^{-11} seconds.

Acknowledgments. -- We acknowledge the useful comments from A.W. Overhauser and M. Nechtschein regarding several aspects of the work described here. This report is based upon work supported by NSF grant DMR-8409390 (WGC and KG) and NSF grant DMR-8121394 (GM).

REFERENCES

*Present address: Physics Dept., Univ. of Illinois at Urbana-Champaign, Urbana, IL. 61801

1. W.P. Su, J.R. Schrieffer, and M.J. Heeger, Phys. Rev. Lett. 42, 1968(1979); M.J. Rice, Phys. Lett. 71A, 152(1979).
2. K. Holczer, F. Devreux, M. Nechtschein, and J.P. Travers, Solid State Commun. 39, 881(1981); M. Nechtschein, F. Devreux, R. L. Green, T.C. Clarke, and G.B. Street, Phys. Rev. Lett. 44, 356 (1980).
3. W.G. Clark, K. Glover, G. Mozurkewich, C.T. Murayama, J. Sanny, S. Etemad, and M. Maxfield, J. Phys. (Paris) Suppl. 44, C3-239(1983).
4. C.D. Jeffries, Dynamic Nuclear Polarization (Interscience Publishers, New York, 1963).
5. J.P. Boucher, S. Ferrieu, and M. Nechtschein, Phys. Rev. B9, 3871(1974), references cited therein.
6. M. Nechtschein, F. Devreux, F. Genoud, M. Gugliemi, and K. Holczer, Phys. Rev. B27,61(1983).
7. N.S. Shiren, Y. Tomkiewicz, H. Thomann, L. Dalton, and T.C. Clarke, J. Phys. (Paris) Suppl. 44, C3-223(1983).
8. B.R. Weinberger, E. Ehrenfreund, A. Pron, A.J. Heeger, and A.G. MacDiarmid, J. Chem. Phys. 72, 4749(1980).
9. K. Mizoguchi, K. Kume, and H. Shirakawa, Solid State Commun. 50, 213(1984).
10. M. Nechtschein, F. Devreux, F. Genoud, M. Guglielmi, and K. Holczer, J. Phys. (Paris) Suppl. 44, C3-209(1983).